International Journal of Dynamics and Control (2022) 10:69–85
https://doi.org/10.1007/s40435-021-00795-3

Dynamic behavior and bifurcation analysis of a deterministic and stochastic coupled logistic map system

S. M. Salman[1] · A. M. Yousef[2] · A. A. Elsadany[3,4]

Received: 11 January 2021 / Revised: 22 March 2021 / Accepted: 27 March 2021 / Published online: 9 April 2021

Abstract
In the present work, a system of two linear coupled logistic map is studied. Local stability analysis of the fixed points of the proposed system is investigated. The system occurs transcritical, flip, and Neimark-Sacker bifurcations, which are analyzed by both center manifold theory and bifurcation theory. For any non-linear system that represents a real-world model affected by noise, white noise is included in the system and its effect on fixed points is analyzed via the technique of stochastic sensitivity function. The phenomenon of noise-induced transitions between closed invariant curves is discussed. Finally, numerical simulations are performed with the aid of Matlab to assure the agreements with analytical results obtained.

Keywords Coupled logistic maps · Fixed points · Bifurcation · White noise · Stochastic sensitivity function

AMS Subject Classifications 39A30 · 39A50 · 37C25 · 34C05 · 93D15

1 Introduction

It is well known that the logistic map is a very simple one-dimensional discrete system that exhibits very complicated behavior through a period-doubling bifurcation cascade and eventual emergence of chaos [1–6]. The celebrated logistic map is given by

$$x_{n+1} = ax_n(1 - x_n), \quad n = 0, 1, 2, 3, \ldots, \tag{1}$$

where $0 < x < 1$, and $0 < a < 4$. Following the formulation of Eq. (1), many researchers have studied different aspects of chaos in two-dimensional logistic map and investigated their applications in many fields [7–9]. Recently, an experimental study of coupled oscillators shows an increase of complexity due to coupling process [10]. Actually, when a system is composed of many nonlinear units, it forms a new complex system with more complex behaviors which are not held by the individual units. Indeed, one of the standard models for nonlinear dynamical systems is to deal with a system of two symmetrically coupled maps admitting move towards chaos via period doubling bifurcations [11–17]. Most of the experimental results that studied systems of coupled objects agree with the complicated dynamical behaviors of coupled systems [18–21]. The two logistic mapping system was applied as a model for the chemical reaction dynamics [22] and population dynamics [23]. Mathematically, there are two ways to couple two logistic maps: linear and bilinear coupling. These types of coupled logistic maps have been studied numerically and analytically [24,25] in which the authors found a quasi-periodic behavior with frequency locking as well as bifurcations. Indeed, discrete dynamical systems (mappings) have attracted the attentions of many researches in the last few decades as they are of enormous relevance in biological and physical processes [26–34]. In addition, discrete time models reflect much richer dynamics than those detected in their continuous temporal counterparts, as they represent many real phenomena in communications, economics and biological sciences.

✉ A. A. Elsadany
aelsadany1@yahoo.com

1 Mathematics Department, Faculty of Education, Alexandria University, Alexandria, Egypt

2 Mathematics Department, Faculty of Science, South valley University, Qena, Egypt

3 Mathematics Department, College of Sciences and Humanities in Al-Kharj, Prince Sattam Bin Abdulaziz University, Al-Kharj 11942, Saudi Arabia

4 Basic Science Department, Faculty of Computers and Informatics, Suez Canal University, Ismailia 41522, Egypt

The field of encryption research is an important field in computer science for the preservation of important information and confidential information, so that information security using hybrid chaotic dynamics has become an important subject that attracts many researchers. The method of encryption on the basis of separate chaotic systems is proposed in [35,36]. In fact, chaotic maps have been shown to have several significant advantages in relation to the basic requirements for encryption algorithms [37]. It is evident from this that discreet logistic maps showing chaotic dynamics or hybrid with any integral transformations or elliptical curves can be very useful in terms of secure communication, encryption and information security.

It's quite well known the uncontrolled random disturbances are an inevitable attribute of any kind of realistic system. The weak noise with a nonlinear system can also dramatically change its dynamics. Analyzing the effect of random disturbances is therefore a challenge for modern dynamics theory in various fields of science, such as biological, engineering and economics. Thus, noise becomes an essential component of the evolution of the dynamic system. It is noted that there is a fundamental shift in the dynamics of coupled systems due to random noise. The effect of noise on the non-linear dynamic behavior of many coupled maps with different goals has been discussed in [38–41].

In this paper, a symmetrically coupled logistic map is considered as follows

$$\begin{cases} x_{n+1} = ax_n(1-x_n) + b(y_n - x_n), \\ y_{n+1} = ay_n(1-y_n) + b(x_n - y_n), \end{cases} \tag{2}$$

where $0 < x_n, y_n < 1$, $0 < a < 4$, and $-2 \le b \le 2$ is called connection parameter. The system (2) is symmetrical with respect to the exchange of x and y and was represented in [25]. Other researchers have reconsidered the system (2) in [42,43].

In this paper, a itemized bifurcation analysis for system (2) is carried out which is not addressed in [25,42,43]. The key contributions and outcomes of this work are defined as follows: It provides a first, thoroughly analytical study of the various types of codimension—one bifurcation that can occur in the linear coupled logistic map (2). Analyzing the effects of white noise on the dynamic behavioral of the system is discussed both analytically and numerically. The system (2) has a number of periodic cycles, such as transcritical, flip, and Neimark-Sacker bifurcations, which are analyzed by both center and bifurcation theories. These are interesting dynamic behaviors that have not been analytically analyzed in the literature for this system. In addition, the impact of each white noise parameter on the dynamic behavior was examined. Moreover, the extensive simulation results will be presented to detect the effect of the parameters on the change of the stability and bifurcation thresholds.

The paper is structured as follows. Section 2 discusses the existence and stability of fixed points of the deterministic system. In Sect. 3, a detailed bifurcation analysis is investigated. A white noise is added to the system and its influence is discussed in Sect. 4. In Sect. 5, some numerical simulations are performed using Matlab to verify the analytical results obtained in Sect. 3. Finally, the conclusion and discussion can be found in Sect. 6.

2 The existence of fixed points and their stability

At most, the system (2) has four fixed points:

1. The fixed point $E_1 = (0, 0)$ exists for all parameters values.
2. For $a \neq 1$, there exists $E_2 = (\frac{a-1}{a}, \frac{a-1}{a})$,
3. Furthermore, there are two fixed points

$$E_3 = \left(\frac{1}{2a}((a-1-2b) + \sqrt{(1-a+2b)(1-a-2b)}), \right.$$
$$\left. \frac{1}{2a}((a-1-2b) - \sqrt{(1-a+2b)(1-a-2b)} \right),$$
$$E_4 = \left(\frac{1}{2a}((a-1-2b) - \sqrt{(1-a+2b)(1-a-2b)}), \right.$$
$$\left. \frac{1}{2a}((a-1-2b) + \sqrt{(1-a+2b)(1-a-2b)} \right),$$

which are real if and only if $a \le 1-2|b|$ or $a \ge 1+2|b|$.

Lemma 1 [44] *Let $F(\lambda) = \lambda^2 + P\lambda + Q$. Suppose that $F(1) > 0$, λ_1 and λ_2 are two roots of $F(\lambda) = 0$. Then*

1. *$|\lambda_1| < 1$ and $|\lambda_2| < 1$ if and only if $F(-1) < 0$, $Q < 1$;*
2. *$|\lambda_1| < 1$ and $|\lambda_2| > 1$ (or $|\lambda_1| > 1$ and $|\lambda_2| < 1$) if and only if $F(-1) < 0$;*
3. *$|\lambda_1| > 1$ and $|\lambda_2| > 1$ if and only if $F(-1) > 0$ and $Q > 1$;*
4. *$\lambda_1 = -1$ and $|\lambda_2| \neq 1$ if and only if $F(-1) = 0$ and $P \neq 0, 2$;*
5. *λ_1 and λ_2 are complex and $|\lambda_1| = 1$and $|\lambda_2| = 1$ if and only if $P^2 - 4Q < 0$ and $Q = 1$.*

Lemma 2 [44] *Let $F(\lambda) = \lambda^2 + P\lambda + Q$ is characteristic equation corresponding with the Jacobian matrix computed at a fixed point (x^*, y^*), then (x^*, y^*) is called*

1. *a sink if $|\lambda_1| < 1$ and $|\lambda_2| < 1$, so the sink is locally asymptotically stable;*
2. *a source if $|\lambda_1| > 1$ and $|\lambda_2| > 1$, so the source is locally unstable;*

3. *a saddle if* $|\lambda_1| > 1$ *and* $|\lambda_2| < 1$ *(or* $|\lambda_1| < 1$ *and* $|\lambda_2| > 1$*);*
4. *non-hyperbolic if either* $|\lambda_1| = 1$ *or* $|\lambda_2| = 1$.

In order to study stability and bifurcation, it is necessary to calculate the Jacobin matrix of the system (2) at any fixed point (x^*, y^*) reads as

$$J(x^*, y^*) = \begin{pmatrix} a(1-2x)-b & b \\ b & a(1-2y)-b \end{pmatrix}. \tag{3}$$

3 Analysis of local bifurcations

A more detailed description of the bifurcation in this section is being performed for the fixed points of system (2). Both center manifold theorem and bifurcation theory [45–50] are used to study bifurcation types in the system (2).

Proposition 1 *The fixed point* $E_1 = (0, 0)$ *of system* (2) *is*

1. *A sink if* $-1 < a < 1$, *and* $\frac{a-1}{2} < b < \frac{a+1}{2}$,
2. *A source if (i)* $a > 1$ *or* $a < -1$ *and (ii)* $b < \frac{a-1}{2}$ *or* $b > \frac{a+1}{2}$,
3. *A saddle if (i)* $a > 1$ *or* $a < -1$ *and (ii)* $\frac{a-1}{2} < b < \frac{a+1}{2}$,
4. *A non-hyperbolic if (i)* $a = \pm 1$ *and (ii)* $b = \frac{a-1}{2}$ *or* $b = \frac{a+1}{2}$.

Proposition 2 *The fixed point* $E_2 = (\frac{a-1}{a}, \frac{a-1}{a})$ *of system* (2) *is*

1. *A sink if* $1 < a + 2b < 3$, *and* $1 < a < 3$,
2. *A source if (i)* $a + 2b < 1$ *or* $a + 2b > 1$ *and (ii)* $1 < a < 3$,
3. *A saddle if* $2ab - 6(a + b) < -5$,
4. *A non-hyperbolic if (i)* $3(a+b)-ab = \frac{5}{2}$ *and (ii)* $a+b \notin \{-2, 1\}$.

It is worth to mention here that system (2) admits no bifurcation at $E_1(0, 0)$.

3.1 Bifurcation of the fixed point E_2

The Jacobian matrix (4) at E_2 reads as

$$J(E_2) = \begin{pmatrix} -a-b+2 & b \\ b & -a-b+2 \end{pmatrix},$$

it owns two eigenvalues $\lambda_1 = -a-2b+2$ and $\lambda_2 = -a+2$. If $a + 2b = 3$, thus we have $\lambda_1 = -1$, $|\lambda_2| \neq 1$ provided that $a \neq 1, 3$.

Theorem 1 *If* $b = \frac{3-a}{2}$, *and* $a \neq 1, 3$, *then system* (2) *exhibits a flip bifurcation at* E_2. *In addition, at this fixed point the stable period-doubling orbit bifurcates.*

Proof The system (2) can be used as follows

$$\begin{cases} x \to ax(1-x) + b(y-x), \\ y \to ay(1-y) + b(x-y). \end{cases} \tag{4}$$

Let b^* is a parameter bifurcation, consider the perturbation of (4) is given by

$$\begin{cases} x \to ax(1-x) + (b+b^*)(y-x), \\ y \to ay(1-y) + (b+b^*)(x-y), \end{cases} \tag{5}$$

which $|b^*| \ll 1$ is a small perturbation.

Consider $u = x - x^*$, $v = y - y^*$, thus map (5) changed as follows

$$\begin{cases} u \to (-a+2-b)u + bv - ub^* + vb^* - au^2 \\ \qquad +O((|u| + |v| + |b^*|)^3), \\ v \to bu + (-a+2-b)v + ub^* - vb^* - av^2 \\ \qquad +O((|u| + |v| + |b^*|)^3). \end{cases} \tag{6}$$

Constructing an invertible matrix as follows

$$T = \begin{pmatrix} b & b \\ a+b-3 & b \end{pmatrix},$$

We use the transformation as follows

$$\begin{pmatrix} u \\ v \end{pmatrix} = T \begin{pmatrix} \tilde{x} \\ \tilde{y} \end{pmatrix},$$

then the system (6) will be changed to

$$\begin{pmatrix} \tilde{x} \\ \tilde{y} \end{pmatrix} \to \begin{pmatrix} -1 & 0 \\ 0 & -a+2 \end{pmatrix} \begin{pmatrix} \tilde{x} \\ \tilde{y} \end{pmatrix} + \begin{pmatrix} \phi(\tilde{x}, \tilde{y}, b^*) \\ \psi(\tilde{x}, \tilde{y}, b^*) \end{pmatrix}, \tag{7}$$

where

$$\begin{aligned} &\phi(\tilde{x}, \tilde{y}, b^*) \\ &\quad = \frac{1}{3-a}\left(-ub^* + vb^* - au^2 + O((|u| + |v| + |b^*|)^3)\right), \\ &\psi(\tilde{x}, \tilde{y}, b^*) \\ &\quad = \frac{1}{b(3-a)}\big((3-a-b)(-ub^* + vb^* - au^2 + bub^* \\ &\quad -bvb^* - abv^2 + O((|u| + |v| + |b^*|)^3)\big). \end{aligned}$$

and

$$\begin{aligned} u &= b(\tilde{x} + \tilde{y}), \\ v &= (a-b-3)\tilde{x} + b\tilde{y}. \end{aligned}$$

By the center manifold theorem [50,51], there exists a center manifold $W_c(0,0,0)$ of (7) at the fixed point $(0,0)$ in a small neighborhood of b^* which may take the form

$$W_c(0,0,0) = \{(\tilde{x},\tilde{y},b^*) \in R^3, \tilde{y} = h(\tilde{x},b^*), h(0,0)=0, Dh(0,0)=0\},$$

for $\tilde{x}$ and δ^* sufficiently small. We suppose that the center manifold of the form

$$h(\tilde{x},b^*) = \mu_0\tilde{x}^2 + \mu_1\tilde{x}b^* + \mu_2 b^{*2} + O((|\tilde{x}|+|b^*|)^3). \quad (8)$$

The center manifold should achieve the equation

$$h(-\tilde{x}+\phi(\tilde{x},h(\tilde{x},b^*),b^*),b^*) = (-a+2)h(\tilde{x},b^*) + \psi(\tilde{x},h(\tilde{x},b^*),b^*). \quad (9)$$

By replacing (8) for (9) and matching similar power coefficients for (9), we obtain

$$\mu_0 = \frac{ab}{(a-1)(a-3)},$$
$$\mu_1 = \frac{a+b-3}{b(a-3)},$$
$$\mu_2 = 0.$$

Hence, we realize the system (7) which is restrictive to the center manifold:

$$F:\tilde{x} \to -\tilde{x} + A\tilde{x}^2 + B\tilde{x}b^* + C\tilde{x}^2b^* + D\tilde{x}b^{*2} + E\tilde{x}^3 + F0\tilde{x}^3b^* + G\tilde{x}^2b^{*2} + H\tilde{x}^4 + O((|\tilde{x}|+|b^*|)^4), \quad (10)$$

where

$$A = \frac{-ab^2}{3-a}, \quad B = \frac{-1}{3-a},$$
$$C = \frac{ab}{(3-a)(a-1)(a-3)} + \frac{ab^2}{(a-1)(a-3)} + \frac{(-2ab^2)(a+b-3)}{b(a-3)(3-a)},$$
$$D = \frac{a+b-3}{b(3-a)(a-3)}, \quad E = \frac{-2a^2b^3}{(a-1)(a-3)(3-a)},$$
$$F0 = \frac{(-2a^2b^3)(a+b-3)}{b(a-3)(3-a)}, \quad G = \frac{(-ab^2)(a+b-3)^2}{b^2(a-3)^2(3-a)},$$
$$H = \frac{-a^2b^3}{(a-1)^2(a-3)^2(3-a)}$$

To allow the map (10) to occur a flip bifurcation, we order that two preferential quantities α_1 and α_2 are not zero [51]:

$$\alpha_1 = \left(2\frac{\partial^2 F}{\partial b^*\partial\tilde{x}} + \frac{\partial F}{\partial b^*}\frac{\partial F}{\partial\tilde{x}}\right)_{(0,0)} = -2 \neq 0,$$

$$\alpha_2 = \left(\frac{1}{2}\left(\frac{\partial^2 F}{\partial\tilde{x}^2}\right)^2 + \frac{1}{3}\left(\frac{\partial^3 F}{\partial\tilde{x}^3}\right)\right)_{(0,0)} = \frac{-2a^2b^4}{3-a}\left(1+\frac{2ab}{(a-1)(a-3)}\right)^2 - \frac{4a^2b^3}{3(3-a)(a-1)(a-3)}\left(1+\frac{2ab}{(a-1)(a-3)}\right) \neq 0.$$

□

Now we discuss the transcritical bifurcation of E_2.

Theorem 2 *If $b = \frac{1-a}{2}$, and $a \neq 1, 3$, then system (2) shows a transcritical bifurcation at E_2.*

Proof Use the b^* as a bifurcation parameter, and realize the disturbance of (4) as in the system (5). Taking $u = x - x^*$, $v = y - y^*$, then the map (5) has form

$$\begin{cases} u \to (1+b)u + bv - ub^* + vb^* - (1-2b)u^2 \\ \qquad +O((|u|+|v|+|b^*|)^3), \\ v \to bu + (1+b)v + ub^* - vb^* - (1-2b)v^2 \\ \qquad +O((|u|+|v|+|b^*|)^3). \end{cases} \quad (11)$$

Design the inverse matrix as follows

$$T = \begin{pmatrix} b & b \\ -b & b \end{pmatrix},$$

and to use transformation

$$\begin{pmatrix} u \\ v \end{pmatrix} = T\begin{pmatrix} \tilde{x} \\ \tilde{y} \end{pmatrix},$$

thus (11) turn into

$$\begin{pmatrix} \tilde{x} \\ \tilde{y} \end{pmatrix} \to \begin{pmatrix} 1 & 0 \\ 0 & \lambda_2 \end{pmatrix}\begin{pmatrix} \tilde{x} \\ \tilde{y} \end{pmatrix} + \begin{pmatrix} \theta(\tilde{x},\tilde{y},b^*) \\ \vartheta(\tilde{x},\tilde{y},b^*) \end{pmatrix}, \quad (12)$$

where

$$\theta(\tilde{x},\tilde{y},b^*) = \frac{1}{2b}(-2ub^* + 2vb^* - (1-2b)(u^2+v^2)) + O((|u|+|v|+|b^*|)^3)),$$
$$\vartheta(\tilde{x},\tilde{y},b^*) = \frac{-(1-2b)}{2b}(u^2+v^2) + O((|u|+|v|+|b^*|)^3)),$$

with

$$u = b(\tilde{x}+\tilde{y}),$$
$$v = b(-\tilde{x}+\tilde{y}).$$

Assuming there is a center manifold $W_c(0,0,0)$ of (12) at the fixed point $(0,0)$ in a small neighborhood of b^* which may take the form

$$W_c(0,0,0) = \{(\tilde{x},\tilde{y},b^*) \in R^3,$$

$$\tilde{y} = l(\tilde{x}, b^*), l(0,0) = 0, Dl(0,0) = 0\},$$

for $\tilde{x}$ and b^* sufficiently small. Consider a center manifold as follows

$$l(\tilde{x}, b^*) = m_0\tilde{x}^2 + m_1\tilde{x}b^* + m_2{b^*}^2 + O((|\tilde{x}| + |b^*|)^3). \quad (13)$$

The center manifold must be satisfied

$$l(\tilde{x} + \theta(\tilde{x}, l(\tilde{x}, b^*), b^*), b^*) = \lambda_2 l(\tilde{x}, b^*) + \vartheta(\tilde{x}, l(\tilde{x}, b^*), b^*). \quad (14)$$

By replacing (13) for (14) and matching similar power coefficients for in (14), we obtain

$$m_0 = \frac{-2(1-2b)}{1-\lambda_2}, m_1 = m_2 = 0.$$

Hence, we realize the system (12) which is restricted to the center manifold:

$$F_1 : \tilde{x} \to \tilde{x} - b(1-2b)\tilde{x}^2 - 2\tilde{x}b^* - b(1-2b)m_0^2\tilde{x}^4 + O((|\tilde{x}| + |b^*|)^5), \quad (15)$$

one can check that conditions of transcritical bifurcation are satisfies as

$$F_1(0,0) = 0, \left(\frac{\partial F_1}{\partial \tilde{x}}\right)_{(0,0)} = 1, \left(\frac{\partial^2 F_1}{\partial \tilde{x}^2}\right)_{(0,0)} = -2b(1-b) \neq 0, \left(\frac{\partial^2 F_1}{\partial b^* \partial \tilde{x}}\right)_{(0,0)} = -2 \neq 0.$$

□

3.2 Bifurcation for the fixed point E_3

The characteristic equation at the positive fixed point $E_3(x^*, y^*) = (\frac{1}{2a}((a-1-2b) + \sqrt{(1-a+2b)(1-a-2b)}), \frac{1}{2a}((a-1-2b) - \sqrt{(1-a+2b)(1-a-2b)})$ has the following form:

$$\lambda^2 + P(x^*, y^*)\lambda + Q(x^*, y^*) = 0,$$

where

$$P(x^*, y^*) = -2a + 2a(x^* + y^*) + 2b,$$
$$Q(x^*, y^*) = a^2(1-2x^*)(1-2y^*) - b(2a - 2a(x^* + y^*)),$$

let

$$F(\lambda) = \lambda^2 + P(x^*, y^*)\lambda + Q(x^*, y^*),$$

If $a > 1 + 2b$, then

$$F(1) = 4b^2 - (1-a)^2 > 0, \qquad F(-1) = 4 + 4b + 4b^2 - (1-a)^2$$

It is very important here to pay attention that we cannot use Lemma 1 to classify topological properties of the fixed points E_3 and E_4. To make this clear, we need for Lemma 1 that $F(1) > 0$ which ends up with $4b^2 - (1-a)^2 > 0$. The last inequality contradicts with the condition $4b^2 - (1-a)^2 < 0$ which is necessary for the fixed points E_3 and E_4 to be real.

Now, by solving the characteristic equation

$$\lambda^2 - 2(1+b)\lambda + (1 + 2b + 4b^2 - (1-a)^2) = 0,$$

has two eigenvalues:

$$\lambda_{1,2} = (1+b) \pm \sqrt{(1-a^2) - 3b^2}. \quad (16)$$

Proposition 3 *The fixed point E_3 of the system (2) is*

- *a sink if $|(1+b) + \sqrt{(1-a^2) - 3b^2}| < 1$, and $|(1+b) - \sqrt{(1-a^2) - 3b^2}| < 1$,*
- *a source if $|(1+b) + \sqrt{(1-a^2) - 3b^2}| > 1$, and $|(1+b) - \sqrt{(1-a^2) - 3b^2}| > 1$,*
- *a saddle if either: $|(1+b) + \sqrt{(1-a^2) - 3b^2}| < 1$, and $|(1+b) - \sqrt{(1-a^2) - 3b^2}| > 1$, or $|(1+b) + \sqrt{(1-a^2) - 3b^2}| > 1$, and $|(1+b) - \sqrt{(1-a^2) - 3b^2}| < 1$,*
- *a non-hyperbolic if either $a = 1 \pm 2|b|$, or $a = 1 \pm 2\sqrt{b^2 + b + 1}$, $b \neq -1, -2$.*

Let

$$FB_1 = \left\{(a,b) : a = 1 - 2\sqrt{(1+b)^2 - b}, b \neq -1, -2\right\},$$

or

$$FB_2 = \left\{(a,b) : a = 1 + 2\sqrt{(1+b)^2 - b}, b \neq -1, -2\right\}.$$

Theorem 3 *The system (2) can admit a flip bifurcation at the fixed point E_3 when parameters vary in a small neighborhood of FB_1 or FB_2.*

Proof Since $(a,b) \in FB_1$, choosing b represents the bifurcation parameter. Assuming the perturbation of (4):

$$\begin{cases} x \to ax(1-x) + (b_1 + b^*)(y - x), \\ y \to ay(1-y) + (b_1 + b^*)(x - y), \end{cases} \quad (17)$$

such that $|b^*| \ll 1$ is the perturbation parameter.

Put $u = x - x^*, v = y - y^*$, thus the map (17) transformed as follows:

$$\begin{cases} u \to a_1 u + a_2 v + a_{13} u b^* + a_{23} v b^* + a_{11} u^2 \\ \quad\quad + O((|u| + |v| + |b^*|)^3), \\ v \to b_1 u + b_2 v + b_{13} u b^* + b_{23} v b^* + b_{22} v^2 \\ \quad\quad + O((|u| + |v| + |b^*|)^3), \end{cases} \tag{18}$$

where

$$\begin{cases} a_1 = a - 2ax^* - b,\ a_2 = b,\ a_{13} \\ = -1,\ a_{23} = 1,\ a_{11} = -a \\ b_1 = b,\ b_2 = a - 2ay^* - b,\ b_{13} \\ = 1,\ b_{23} = -1,\ b_{23} = -1,\ b_{22} = -a. \end{cases} \tag{19}$$

Construct an invertible matrix

$$T = \begin{pmatrix} a_2 & a_2 \\ -1 - a_1 & \lambda_2 - a_1 \end{pmatrix},$$

and applying transformation:

$$\begin{pmatrix} u \\ v \end{pmatrix} = T \begin{pmatrix} \tilde{x} \\ \tilde{y} \end{pmatrix},$$

then the system (18) will be changed to

$$\begin{pmatrix} \tilde{x} \\ \tilde{y} \end{pmatrix} \to \begin{pmatrix} -1 & 0 \\ 0 & \lambda_2 \end{pmatrix} \begin{pmatrix} \tilde{x} \\ \tilde{y} \end{pmatrix} + \begin{pmatrix} f(\tilde{x}, \tilde{y}, b^*) \\ g(\tilde{x}, \tilde{y}, b^*) \end{pmatrix},$$

where

$$\begin{aligned} f(\tilde{x}, \tilde{y}, b^*) = & \left(\frac{a_{13}(\lambda_2 - a_1)}{a_2(1 + \lambda_2)} - a_2 b_{13} \right) u b^* \\ & + \left(\frac{a_{23}(\lambda_2 - a_1)}{a_2(1 + \lambda_2)} - a_2 b_{23} \right) v b^* \\ & + \frac{a_4(\lambda_2 - a_1)}{a_2(1 + \lambda_2)} u^2 - \frac{a_2 b_{22}}{a_2(1 + \lambda_2)} v^2 \\ & + O((|u| + |v| + |b|^*|)^3), \\ g(\tilde{x}, \tilde{y}, b^*) = & \left(\frac{(1 + a_1) a_{13}}{a_2(1 + \lambda_2)} + a_2 b_{13} \right) u b^* \\ & + \left(\frac{(1 + a_1) a_{23}}{a_2(1 + \lambda_2)} + a_2 b_{13} \right) v b^* \\ & + \frac{(a_1 + 1) a_{11}}{a_2(1 + \lambda_2} u^2 + \frac{a_2 b_{22}}{a_2(1 + \lambda_2} v^2 \\ & + O((|u| + |v| + |b|^*|)^3). \end{aligned}$$

and

$$\begin{aligned} & u = a_2(\tilde{x} + \tilde{y}),\ v = -(1 + a_1)\tilde{x} + (\lambda_2 - a_1)\tilde{y}, \\ & u^2 = a_2^2(\tilde{x}^2 + \tilde{x}\tilde{y} + \tilde{y}^2), \\ & v^2 = (1 + a_2)^2 \tilde{x}^2 + (\lambda_2 - a_1)^2 \tilde{y}^2 - 2(1 + a_1)(\lambda_2 - a_1)\tilde{x}\tilde{y}. \end{aligned}$$

Based on the center manifold theory, there exists the following center manifold:

$$\begin{aligned} W_c(0, 0, 0) = & \{(\tilde{x}, \tilde{y}, b^*) \in R^3, \\ & \tilde{y} = h(\tilde{x}, b^*), h(0, 0) = 0, Dh(0, 0) = 0\}, \end{aligned}$$

for $\tilde{x}$ and b^* sufficiently small. To compute the center manifold, we assume that

$$h(\tilde{x}, b^*) = n_0 \tilde{x}^2 + n_1 \tilde{x} b^* + n_2 b^{*2} + O((|\tilde{x}| + |b^*|)^3). \tag{20}$$

The center manifold has to satisfy

$$\begin{aligned} & h(-\tilde{x} + f(\tilde{x}, h(\tilde{x}, b^*), b^*), b^*) \\ & \quad = \lambda_2 h(\tilde{x}, b^*) + g(\tilde{x}, h(\tilde{x}, b^*), b^*). \end{aligned} \tag{21}$$

Replacing (20) in (21) and matching similar power coefficient values of (21), we have

$$\begin{aligned} n_0 &= \frac{a_{11} a_2 (1 + a_1) + b_{22}(1 + a_1)^2}{(1 - \lambda_2^2)}, \\ n_1 &= \frac{-(1 + a_1) a_{13} - a_2 b_{13}}{(1 + \lambda_2)^2}, \\ n_2 &= 0. \end{aligned}$$

The system (18) constrained by the center manifold is given as follows:

$$\begin{aligned} F_2 : \tilde{x} \to & -\tilde{x} + A_1 \tilde{x}^2 + A_2 \tilde{x} b^* + A_3 \tilde{x}^2 b^* + A_4 \tilde{x} b^{*2} \\ & + A_5 \tilde{x}^3 + A_6 \tilde{x}^3 b^* + A_7 \tilde{x}^2 b^{*2} + A_8 \tilde{x}^4 + O((|\tilde{x}| + |b^*|)^5). \end{aligned} \tag{22}$$

where

$$\begin{aligned} A_1 &= a_{11} a_2^2 - a_2 b_{22}(1 + a_1), \\ A_2 &= \frac{\lambda_2 - a_1}{a_2(1 + \lambda_2)}(a_{13} a_2 - a_{23}(1 + a_1)) \\ &\quad - a_2^2 b_{13} + b_{23} a_2 (1 + a_1), \\ A_3 &= \frac{\lambda_2 - a_1}{a_2(1 + \lambda_2)}(a_{13} a_2 n_0 + a_{23}(\lambda_2 - a_1) n_0 + 2a_{11} a_2^2 n_1) \\ &\quad - a_2^2 b_{13} n_0 - a_2 b_{23}(\lambda_2 - a_1) n_0 \\ &\quad + a_2 b_{22}(1 + a_1)(\lambda_2 - a_1) n_1, \\ A_4 &= \frac{\lambda_2 - a_1}{a_2(1 + \lambda_2)}(a_{13} a_2 n_1 + a_{23}(\lambda_2 - a_1) n_1) \\ &\quad - a_2^2 b_{13} n_1 - a_2 b_{23}(\lambda_2 - a_1) n_1, \\ A_5 &= 2a_{11} a_2^2 n_0 \frac{\lambda_2 - a_1}{a_2(1 + \lambda_2)} + a_2 b_{22}(1 + a_1)(\lambda_2 - a_1) n_0, \\ A_6 &= 2a_{11} a_2^2 n_0 n_1 \frac{\lambda_2 - a_1}{a_2(1 + \lambda_2)} - 2a_2 b_{22}(\lambda_2 - a_1)^2 n_0 n_1, \\ A_7 &= a_{11} a_2^2 n_1^2 \frac{\lambda_2 - a_1}{a_2(1 + \lambda_2)} - a_2 b_{22}(\lambda_2 - a_1)^2 n_1^2, \end{aligned}$$

$$A_8 = a_{11}a_2^2n_0^2\frac{\lambda_2 - a_1}{a_2(1+\lambda_2)} - a_2b_{22}(\lambda_2 - a_1)^2n_0^2.$$

Thus, map (22) undergoes a flip bifurcation because the following conditions are satisfied

$$\beta_1 = \Big(2\frac{\partial^2 F_2}{\partial b^*\partial\tilde{x}} + \frac{\partial F_2}{\partial b^*}\frac{\partial F_2}{\partial\tilde{x}}\Big)_{(0,0)} = 2A_2 \neq 0,$$
$$\beta_2 = \Big(\frac{1}{2}\Big(\frac{\partial^2 F_2}{\partial\tilde{x}^2}\Big)^2 + \frac{1}{3}\Big(\frac{\partial^3 F_2}{\partial\tilde{x}^3}\Big)\Big)_{(0,0)} = 2(A_1^2 + A_5) \neq 0.$$

□

The same procedure can be applied to the points in the neighborhood of FB_2.

We pay attention here that a Neimark-Sacker bifurcation can not occur neither at the fixed point E_3 nor at E_4. This is because the eigenvalues in (16) are complex only if $3b^2 > (1-a)^2$ which contradicts the fact that the fixed points E_3 and E_4 are real only if $4b^2 < (1-a)^2$. On the other hand, we may discuss the possibility of occurence of Neimark-Sacker bifurcation at E_3 if it is not real. If the (a, b) parameters vary in a small neighborhood of $NS_{1,2}$ which is expressed by

$$NS_1 = \left\{(a,b) : b = \frac{-1+\sqrt{1+4(1-a)^2}}{2}, a \neq -1, 3\right\},$$

$$NS_2 = \left\{(a,b) : b = \frac{-1-\sqrt{1+4(1-a)^2}}{2}, a \neq -1, 3\right\},$$

Considering parameters (c, s, b_2) arbitrarily from NS_1, Take into account the system (5) with (c, s, b_2), that is described in

$$\begin{cases} x \to ax(1-x) + b_2(y-x), \\ y \to ay(1-y) + b_2(x-y), \end{cases} \tag{23}$$

The system (23) has a positive fixed point $E_3(x^*, y^*)$. Since parameters $(c, s, b_2) \in NS_1$, then $b_2 = \frac{-1+M}{4}$, where $M = \sqrt{1+4(1-a)^2}$. Choosing b^* as the bifurcation parameter, we consider a perturbation of the system (23) as follows:

$$\begin{cases} x \to ax(1-x) + (b_2 + \bar{b^*})(y-x), \\ y \to ay(1-y) + (b_2 + \bar{b^*})(x-y), \end{cases} \tag{24}$$

such that $\bar{b^*} \ll 1$ is a perturbation parameter.

Let $u = x - x^*$, $v = y - y^*$, thus the map (24) transformed to

$$\begin{cases} u \to & a_1u + a_2v + a_{11}u^2 + O((|u| + |v| + |b^*|)^3), \\ v \to & b_1u + b_2v + b_{22}v^2 + O((|u| + |v| + |b^*|)^3), \end{cases} \tag{25}$$

where a_1, a_2, a_{11}, and b_1, b_2, b_{22} are chosen to give (20) replacing b_1 by $b_2 + \bar{b}^*$.

Now, the characteristic equation of system (25) can be written as

$$\lambda^2 + P(\bar{b}^*)\lambda + Q(\bar{b}^*) = 0,$$

where

$$P(\bar{b}^*) = -2(1 + \bar{b}^* + b_2),$$
$$Q(\bar{b}^*) = 1 + 2(\bar{b}^* + b_2) + 4(\bar{\delta}^* + \delta_2)^2 - (1-a)^2.$$

Now, we can write the pair of complex eigenvalues in the form

$$\lambda, \bar{\lambda} = -\frac{P(\bar{b}^*)}{2} \pm \frac{i}{2}\sqrt{4Q(\bar{b}^*) - P^2(\bar{b}^*)},$$

and so

$$|\lambda|_{\bar{b}^*=0} = \sqrt{Q(0)} = 1,$$
$$\frac{d|\lambda|}{d\bar{b}^*}|_{\bar{b}^*=0} = -\frac{M}{\sqrt{\frac{1}{4}(3+M^2) - (1-a)^2}} \neq 0.$$

Moreover, we required that when $\bar{b}^* = 0$, $\lambda^m, \bar{\lambda}^m \neq 1$, $(m = 1, 2, 3, 4)$, which is equivalent to $P(0) \neq -2, 0, 1, 2$. Since we choose $(c, s, b_2) \in NS_1$. So, $P(0) \neq -2, 2$. We require only that $P(0) \neq 0, 1$, which ends up with

$$M \neq -3, 3. \tag{26}$$

Therefore, the eigenvalues $\lambda, \bar{\lambda}$ at origin of the system (25) do not lie in the intersection of the unit circle with the coordinate axes when $\bar{b}^* = 0$ and the condition (26) holds.

Next, we analyze the normal system form (25) at $\bar{b}^* = 0$. Let $\bar{b}^* = 0$, $\mu = 1 + b_2$, $\omega = \sqrt{3b^2 - (1-a)^2}$. Construct an invertible matrix

$$T = \begin{pmatrix} a_2 & 0 \\ \mu - a_1 & -\omega \end{pmatrix},$$

using transformation

$$\begin{pmatrix} u \\ v \end{pmatrix} = T \begin{pmatrix} \tilde{x} \\ \tilde{y} \end{pmatrix},$$

then the system (25) has form

$$\begin{pmatrix} \tilde{x} \\ \tilde{y} \end{pmatrix} \to \begin{pmatrix} \mu & -\omega \\ \omega & \mu \end{pmatrix} \begin{pmatrix} u \\ v \end{pmatrix} + \begin{pmatrix} f_1(\tilde{x}, \tilde{y}) \\ f_2(\tilde{x}, \tilde{y}) \end{pmatrix}, \tag{27}$$

where

$$f_1(\tilde{x}, \tilde{y}) = \frac{a_{11}}{a_2} u^2 + O((|\tilde{x}| + |\tilde{y}|)^3),$$
$$f_2(\tilde{x}, \tilde{y}) = \frac{(\mu - a_1)a_{11}}{a_2 \omega} u^2 - \frac{b_{22}}{\omega} v^2 + O((|\tilde{x}| + |\tilde{y}|)^3).$$

with

$$u = a_2 \tilde{x}, \ v = (\mu - a_1)\tilde{x} - \omega \tilde{y},$$
$$u^2 = {a_2}^2 \tilde{x}^2, \ v^2 = (\mu - a_1)^2 \tilde{x}^2 + \omega^2 \tilde{y}^2 - 2\omega(\mu - a_1)\tilde{x}\tilde{y}.$$

So, at the origin (0, 0), we have

$$f_{1\tilde{x}\tilde{x}} = 2a_{11}a_2,$$
$$f_{1\tilde{x}\tilde{x}\tilde{x}} = f_{1\tilde{x}\tilde{y}} = f_{1\tilde{y}\tilde{y}} = f_{1\tilde{x}\tilde{x}\tilde{y}} = f_{1\tilde{x}\tilde{y}\tilde{y}} = f_{1\tilde{y}\tilde{y}\tilde{y}} = 0,$$
$$f_{2\tilde{x}\tilde{x}} = \frac{2(\mu - a_1)}{\omega}(a_2 - b_{22}(\mu - a_1)), \ f_{2\tilde{x}\tilde{y}} = b_{22}(\mu - a_1),$$
$$f_{2\tilde{y}\tilde{y}} = -2b_{22}\omega,$$
$$f_{2\tilde{x}\tilde{x}\tilde{x}} = f_{2\tilde{x}\tilde{x}\tilde{y}} = f_{2\tilde{x}\tilde{y}\tilde{y}} = f_{2\tilde{y}\tilde{y}\tilde{y}} = 0.$$

The system (25) will encounter the Neimark-Sacker bifurcation when the following quantity is not equal to zero:

$$\theta = \Big[- Re\Big(\frac{(1 - 2\lambda)\bar{\lambda}^2}{1 - \lambda} L_{11} L_{12}\Big) - \frac{1}{2}|L_{11}|^2 - |L_{21}|^2 + Re(\bar{\lambda} L_{22})\Big]_{\bar{b}^* = 0},$$

where

$$L_{11} = \frac{1}{4}((f_{1\tilde{x}\tilde{x}} + f_{1\tilde{y}\tilde{y}}) + i(f_{2\tilde{x}\tilde{x}} + f_{2\tilde{y}\tilde{y}})),$$
$$L_{12} = \frac{1}{8}((f_{1\tilde{x}\tilde{x}} - f_{1\tilde{y}\tilde{y}} + 2f_{2\tilde{x}\tilde{y}}) + i(f_{2\tilde{x}\tilde{x}} - f_{2\tilde{y}\tilde{y}} - 2f_{1\tilde{x}\tilde{y}})),$$
$$L_{21} = \frac{1}{8}((f_{1\tilde{x}\tilde{x}} - f_{1\tilde{y}\tilde{y}} - 2f_{2\tilde{x}\tilde{y}}) + i(f_{2\tilde{x}\tilde{x}} - f_{2\tilde{y}\tilde{y}} + 2f_{1\tilde{x}\tilde{y}})),$$
$$L_{22} = \frac{1}{16}((f_{1\tilde{x}\tilde{x}\tilde{x}} + f_{1\tilde{x}\tilde{y}\tilde{y}} + f_{2\tilde{x}\tilde{x}\tilde{y}} + f_{2\tilde{y}\tilde{y}\tilde{y}}) + i(f_{2\tilde{x}\tilde{x}\tilde{x}} + f_{2\tilde{x}\tilde{y}\tilde{y}} - f_{1\tilde{x}\tilde{x}\tilde{y}} - f_{1\tilde{y}\tilde{y}\tilde{y}})),$$

The same arguments can be applied to NS_2.

4 Coupled logistic maps with white noise

In any real system, noise is present and this makes the interaction between nonlinearity and stochasticity very important in modeling dynamic behaviors of many systems such as epidemics, climate, optics and so on [52–55]. In [55], the authors have studied the effect of noise on the attractors of two coupled logistic maps. They have concluded that a very small noise can lead to attractor destruction. The aim of this part of the paper is to discuss the response of the fixed points of the deterministic system (2) to random disturbance.

Consider the following stochastically forced system

$$\begin{cases} x_{n+1} = a x_n(1 - x_n) + b(y_n - x_n) + \varepsilon_1 \eta_n, \\ y_{n+1} = a y_n(1 - y_n) + b(x_n - y_n) + \varepsilon_2 \zeta_n, \end{cases} \tag{28}$$

where ε_1 and ε_2 are noise intensities, and η_n and ζ_n are independent Gaussian random values with parameters $E\eta_n = E\zeta_n = 0$, $E\eta^2 = E\zeta^2 = 1$. According to [56], the stochastic trajectories leave the deterministic attractor under the random noise and form a probabilistic distribution nearby. In our analysis, we assume that $\varepsilon_1 = \varepsilon_2 = \varepsilon$.

4.1 Analysis of randomly forced fixed points

As the noise is present, the regular structure of the fixed points is smoothed. A dispersion of random states near the bifurcation points grows. Consider the influence of noise on fixed point E_1 of model (2). The following analysis is based on the stochastic sensitively function technique and confidence ellipses method represented in [56–59]. Let us consider the impact of the noise on E_1. According to this method, we need to construct a matrix $W = \begin{pmatrix} w_{11} & w_{12} \\ w_{21} & w_{22} \end{pmatrix}$, which is the stochastic sensitivity matrix for the fixed point $E_1(0, 0)$. In fact, W is the unique solution to the matrix equation [56] $W = JWJ^T + Q$, $J = \frac{\partial f}{\partial x}(E_1)$, $Q = \sigma(E_1)\sigma^T(E_1)$, where $f = \begin{pmatrix} ax(1 - x) + b(y - x) \\ ay(1 - y) + b(x - y) \end{pmatrix}$, and $\sigma(E_1)$ characterizes the dependence of random disturbance on state. Consequently, we have

$$w_{11} = \frac{-a^2 + 2ab - 2b^2 + 1}{a^4 - 4a^3b + 4a^2b^2 - 2a^2 + 4ab - 4b^2 + 1},$$
$$w_{12} = w_{21} = \frac{2b(a - b)}{a^4 - 4a^3b + 4a^2b^2 - 2a^2 + 4ab - 4b^2 + 1},$$
$$w_{22} = \frac{-a^2 + 2ab - 2b^2 - 1}{a^4 - 4a^3b + 4a^2b^2 - 2a^2 + 4ab - 4b^2 + 1}.$$

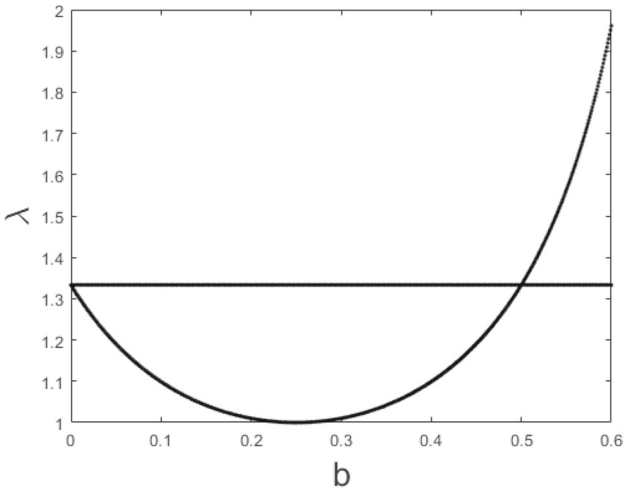

Fig. 1 Eigenvalues of the matrix W of system (28) at E_1

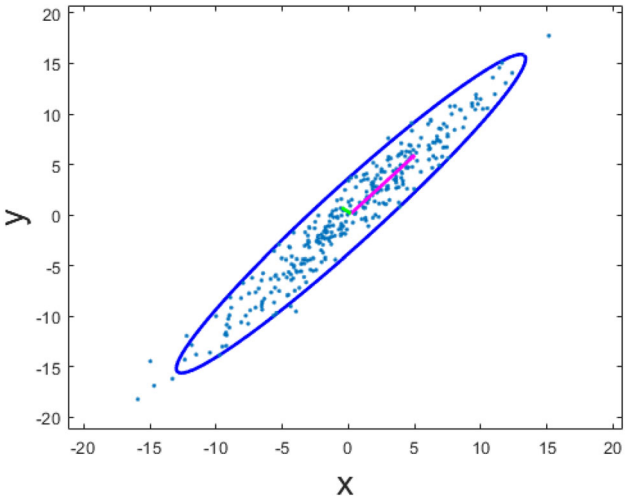

Fig. 2 Random states and confidence ellipse for $a = 0.5$ and $\varepsilon = 0.001$ of the system (28) at E_1

The eigenvalues associated to W are $\lambda_1 = \frac{-1}{a^2-1}$, and $\lambda_2 = \frac{1}{-a^2+4ab-4b^2+1}$ which at the fixed point E_1 describes the stochastic sensitivity of noise.

The two eigenvalues have different attitude as it is depicted in Fig. 1. $\lambda_1(b)$ is constant while $\lambda_2(b)$ is monotonically increasing form 1.35 to 1.95 for $a = 0.5$. These eigenvalues and the corresponding eigenvectors form confidence ellipses as spatial arrangement of random states around the fixed point $E_1(0, 0)$. In fact, the eigenvalues determine the sizes of the semi-axes of the ellipses, and the eigenvectors demonstrate the directions of these axes. Figure 2 shows random states and confidence ellipse for $a = 0.5$, $\varepsilon = 0.001$ and $b = 0.6$ of system (28) at E_1 with a trust probability of $P = 0.95$.

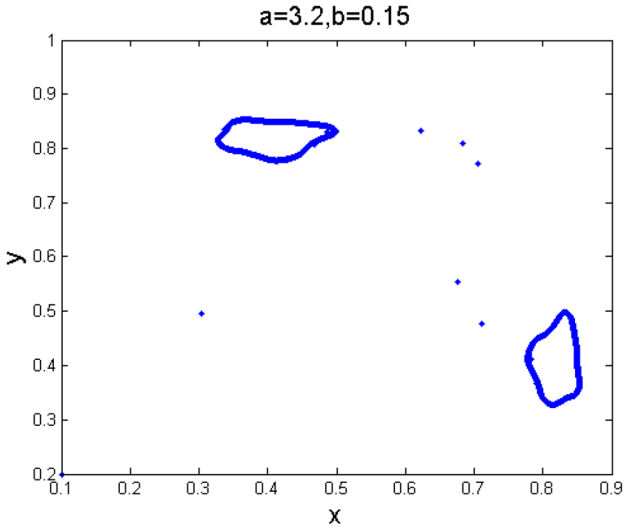

Fig. 3 Attractors of the deterministic system (2) for $a = 3.2$ and $b = 0.15$

4.2 Noise-induced transitions between attractors

The deterministic system (2) has variety of dynamic behavior such as regular attractors deformed in closed invariant curves. Consider the transition induced by noise between stochastic system attractors (28) for $a = 3.2$, and $b = 0.15$. For these values, the deterministic system (2) admits coexisting two closed invariant curves and a 6-discrete cycle as shown in Fig. 3.

First of all, let the noise intensity be weak, that is $\varepsilon = 0.002$. As depicted in Fig. 4, random trajectories which start near one of the closed invariant curves are well localized near it. As the intensity of the noise increases, that is $\varepsilon = 0.02$, a dispersion of random states increases too.

5 Numerical simulations

Numerical simulations for the verification of analytical results obtained in Sects. 3 and 4 are shown in this section.

1. First of all, let us consider the deterministic system (2). Fix the parameter a and let b be free. In Figs. 5 and 6, we present the bifurcation diagram and corresponding maximal lyapunov exponent for the influence of the parameter b. Figure 7 represents the bifurcation diagram when $a = 3$ with initial values $(x_0, y_0) = (0.1, 0.2)$. The fixed point$E_2 = (\frac{a-1}{a}, \frac{a-1}{a})$ is given by $E_2 = (0.6875, 0.6875)$. At $b = -0.1$, E_2 loses its stability via a period-2 orbit that agrees with the theorem 1. The associated maximal lyapunov exponent is shown in Fig. 8. Next, let $a = 3.4$, that is, $E_2 = (0.7059, 0.7059)$. At $b = -0.2$, E_2 loses its stability via a period-2 orbit which

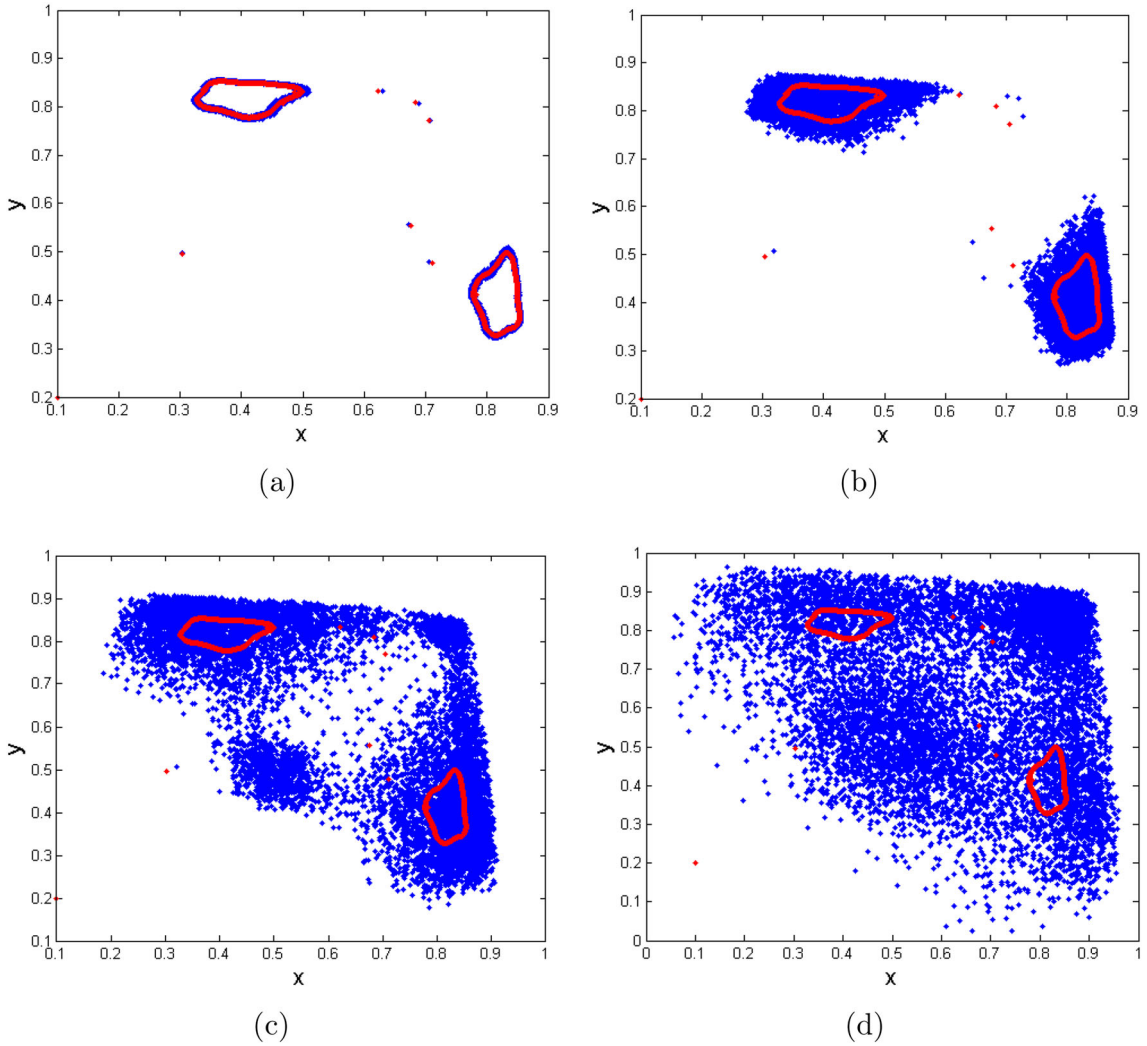

Fig. 4 Random states of system (28) with $a = 3.2$, $b = 0.15$, and a)$\varepsilon = 0.002$, b)$\varepsilon = 0.02$, c)$\varepsilon = 0.05$, d)$\varepsilon = 0.1$, closed invariant curves of system (2) are plotted in red

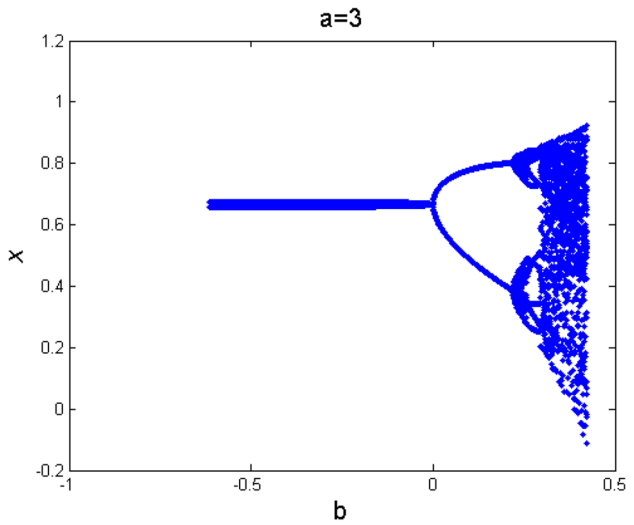

Fig. 5 Bifurcation of (2) in (b, x) plane for $a = 3$

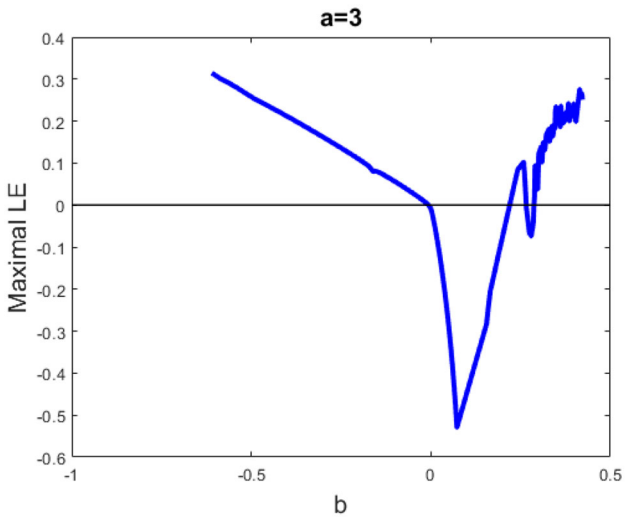

Fig. 6 Maximal Lyapunov exponent for (2)

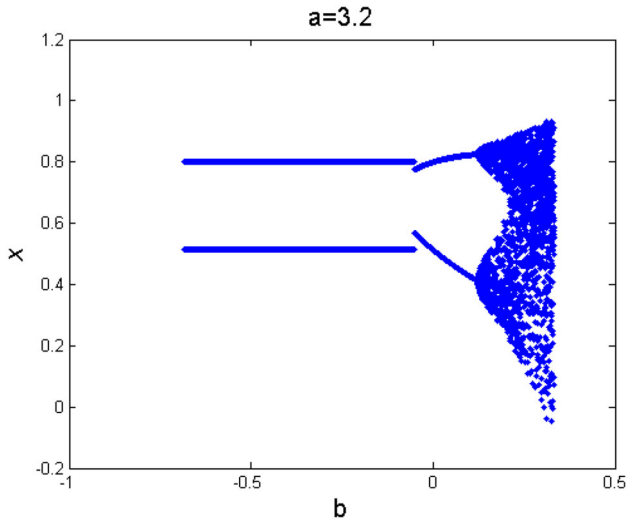

Fig. 7 Bifurcation for the system (2) in (b, x) plane for $a = 3.2$

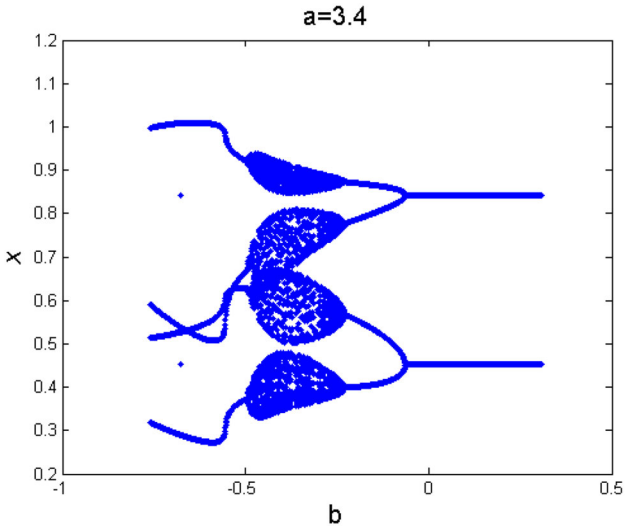

Fig. 9 Bifurcation for the system (2) in (b, x) plane for $a = 3.4$

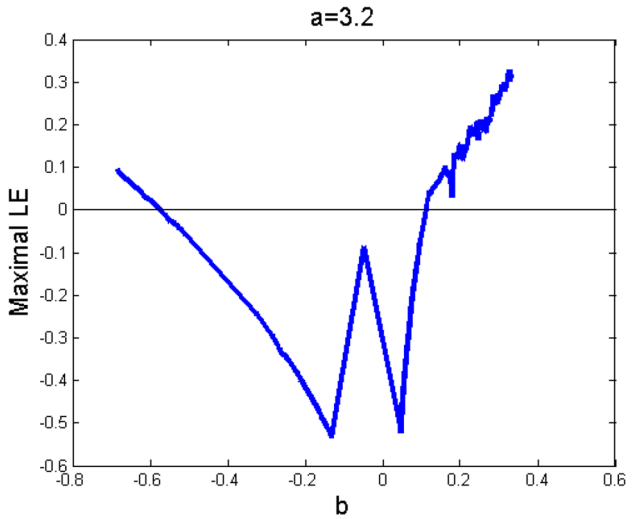

Fig. 8 Maximal Lyapunov exponent for (2)

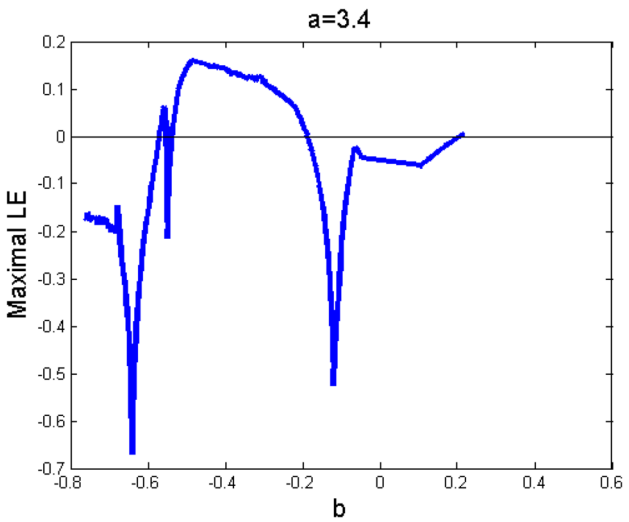

Fig. 10 Maximal Lyapunov exponent for (2)

again agrees with theorem 1 as can be seen in Fig. 9. The corresponding maximal lyapunov exponent is shown in Fig. 10. The same results can be said to Figs. 11 and 12. The transcritical bifurcation at $E_2 = (0.6875, 0.6875)$ occurs at $b = -1.1$ as $a = 3.2$ as can be seen in Fig. 7 which agrees with theorem 2. Again the system (2) admits a transcritical bifurcation at $E_2 = (0.7059, 0.7059)$ if $a = 3.4$ and $b = -1.2$ and this agrees with theorem 2. Figure 11 illustrates the bifurcation diagram for $a = 3.45$ and different b, while Fig. 12 illustrates the corresponding maximal lyapunov exponent. Finally, different phase portraits are plotted in Fig. 13 for different a and b. Figure 13a shows four closed invariant curves with $a = 3.4$ and $b = -0.45$ which appear as a result of a Neimark-Sacker bifurcation, while Fig. 13b–e show chaotic attractors with $a = 3.5, 3.5, 3, 3.2, 3.45, 3.45$ and $b = -0.4, -0.2, 0.4, 0.3, -0.3, -0.25$ respectively. In [43], it was concluded that coupled logistic maps have new transitions to chaos such as quasiperiodicity and torus destruction as can be seen in Figs. 9 and 11.

2. Second of all, let us consider the stochastic system (28). Figure 14 shows the noise induced transformations of bifurcation diagrams for $a = 3.4$ and for $\varepsilon = 0.001, 0.005, 0.02, 0.01$ in Fig. 14a–d, respectively. From above figures, the fine structures of the bifurcation diagrams become blemished especially near the bifurcation points. Fig. 15a–d show the influence of the white noise on the regular attractors (four closed invari-

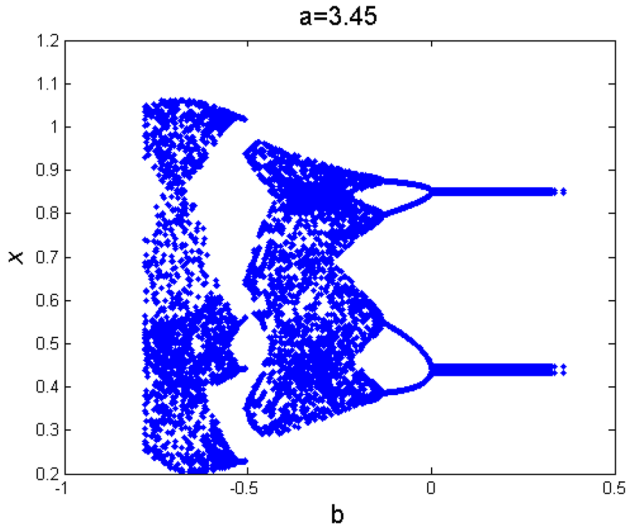

Fig. 11 Bifurcation for the system (2) in (b, x) plane for $a = 1.7$

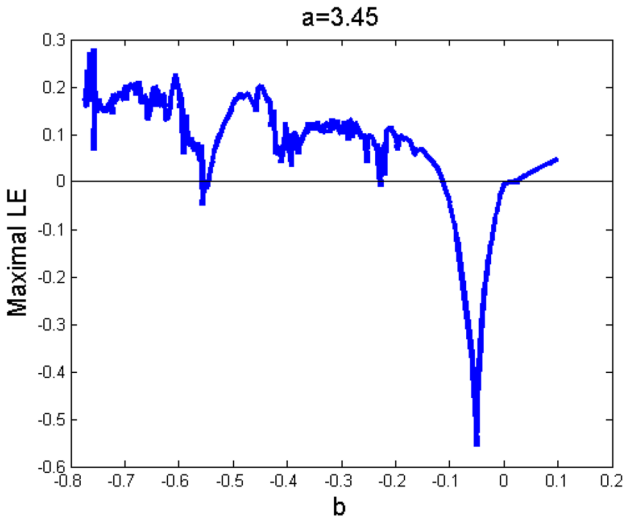

Fig. 12 Maximal Lyapunov exponent for (2)

ant curves here) of the deterministic system (2) when $a = 3.4$, $b = -0.25$ and different noise intensity $\varepsilon = 0.001, 0.005, 0.02, 0.01$.

6 Conclusion

Linearly coupled logistic maps as a deterministic and a stochastic system is considered in this work. The form of the coupled system were already proposed in [25] and investigated further by other researchers but the detailed bifurcation analysis were not reported in any of them. The local stability conditions for the fixed points of the deterministic system are obtained. Dynamic behavior such as bifurcation and chaos is described in the proposed system. According to the center manifold theorem and the bifurcation theory, explicit conditions assure that the system admits transcritical, flip, and Neimark-Sacker bifurcations are given. The detailed bifurcation analysis introduced here supports the numerical observations given in [25]. Since we believe that noise is present in any nonlinear real system, we add a white noise to the deterministic system and study its influence on its fixed points using the stochastic sensitivity function technique. Finally, The phenomenon of noise-induced shifts between closed invariant curves is explored.

Now, the new results in this work enhance the understanding of the complexities of deterministic and stochastic logistic mapping system. The rich dynamics of the system have also been analyzed, including interesting chaotic sets. In addition, the studied system (2) can be used in various engineering applications such as secure communications, encryption and security of information which will be investigated in a forthcoming work. In addition, this paper provides an effective analytical technique for the thorough implementation of various discrete time systems.

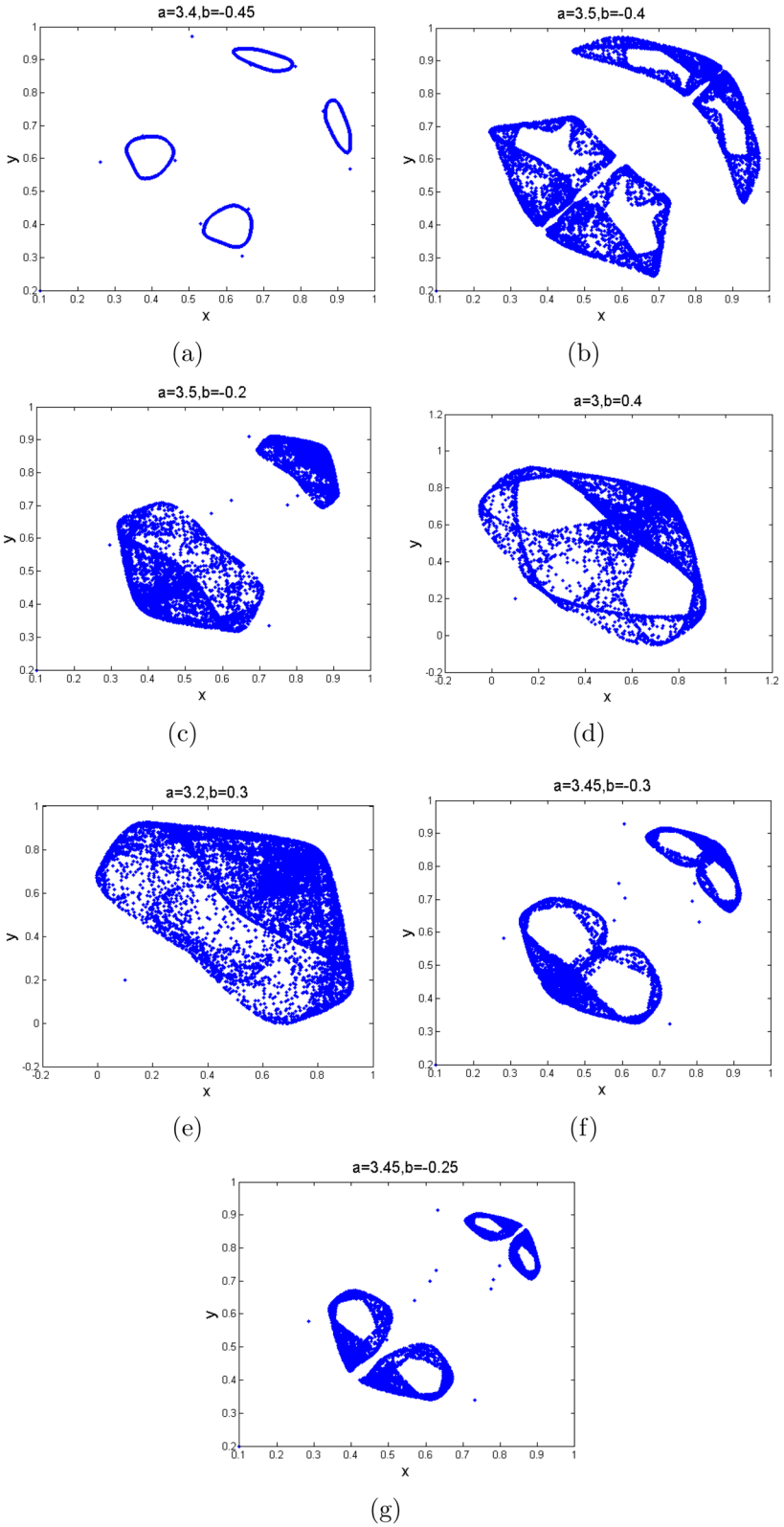

Fig. 13 Phase portraits for the system (2) with different a and b

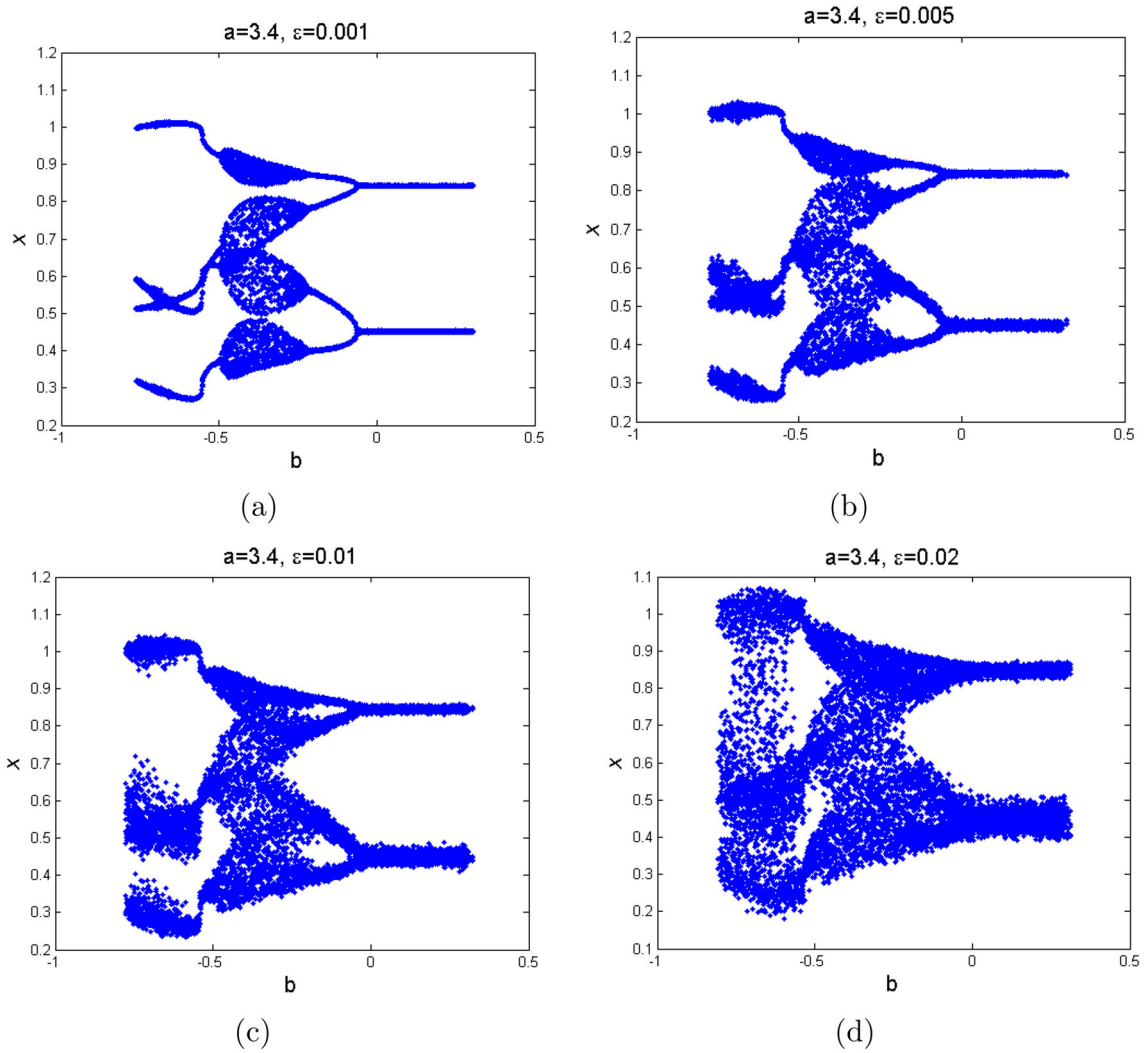

Fig. 14 The bifurcation diagrams for stochastic system (28) with $a = 3.4$ and **a** $\varepsilon = 0.001$, **b** $\varepsilon = 0.005$, **c** $\varepsilon = 0.02$, and **d** $\varepsilon = 0.01$

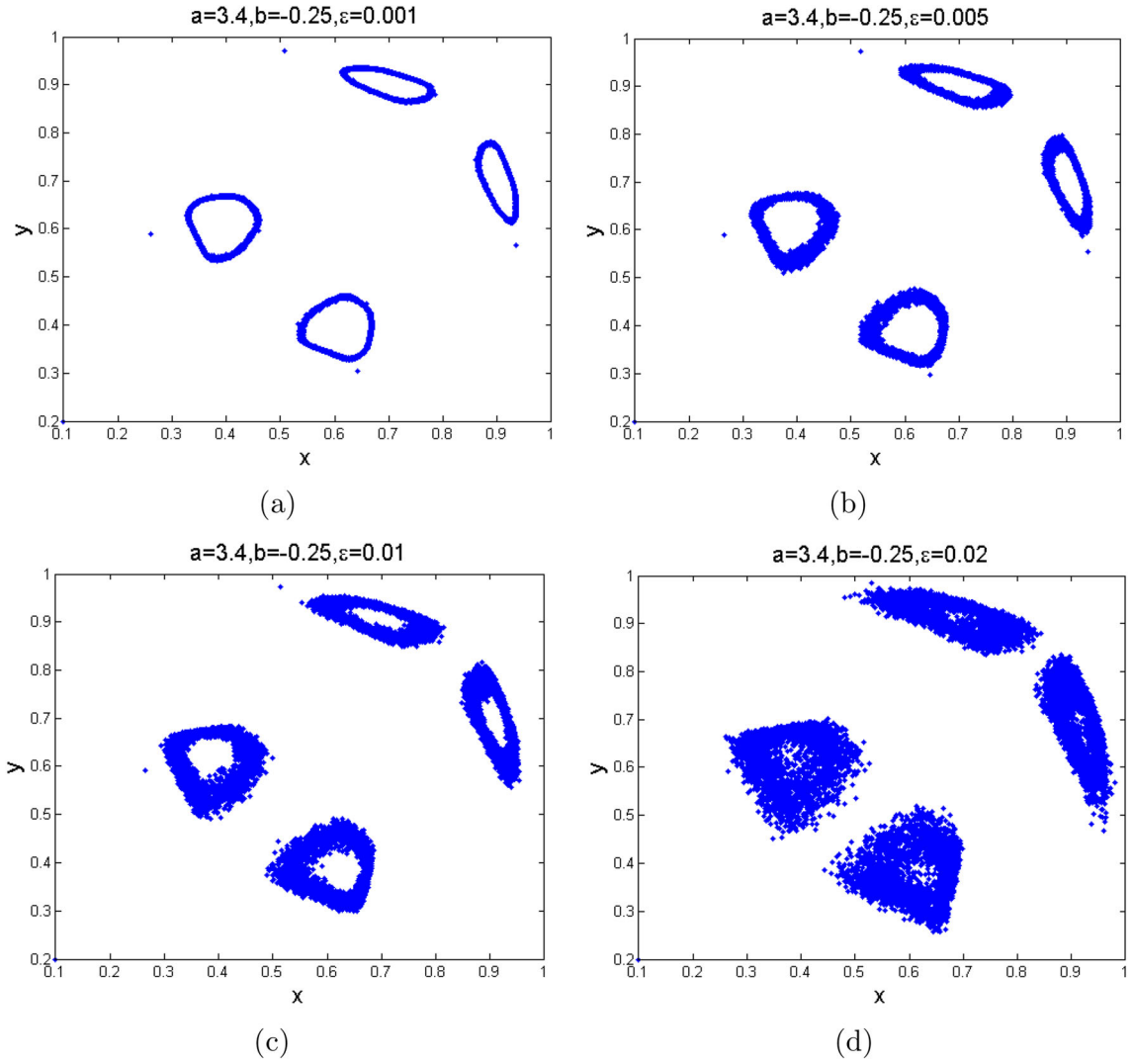

Fig. 15 Phase portraits for the stochastic system (28) with $a = 3.4$, $b = -0.25$, and **a** $\varepsilon = 0.001$, **b** $\varepsilon = 0.005$, **c** $\varepsilon = 0.02$, and **d** $\varepsilon = 0.01$

Acknowledgements We would appreciate the editor and referees for their valuable comments and suggestions to improve our paper. The corresponding author would like to thanks the Prince Sattam bin Abdulaziz University for their support.

Author Contributions All authors contributed equally to the writing of this paper. All authors read and approved the final manuscript.

Availability of data and materials The data used to support the findings of this study are included within the article.

Declarations

Conflict of interest It is declared that none of the authors have any competing interests in this manuscript.

References

1. Hao BL (1993) Starting with parabolas: an introduction to chaotic dynamics. Shanghai Scientific and Technological Education Publishing House, Shanghai
2. Chen SG (1992) Mapping and chaos. National Defence Industry Press, Beijing in Chinese
3. May RM (1976) Simple mathematical models with very complicated dynamics. Nature 261:459–467
4. Feigenbaum MJ (1978) Quantitative universality for a class of nonlinear transformations. J Stat Phys 19:25–52
5. Alligood KT, Sauer TD, Yorke JA (1996) Chaos: an introduction to dynamical systems. Springer, New York
6. Collet P, Eckmann JP (2009) Iterated Maps on the Interval as Dynamical Systems. Springer, New York
7. Yue W, Gelan Y, Huixia J, Noonana JP (2012) Image encryption using the two-dimensional logistic chaotic map. J Electron Imaging 21:1–15
8. Xing-Yuan W, Ying-Qian Z, Yuan-Yuan Z (2015) A novel image encryption scheme based on 2-D logistic map and DNA sequence operations. Nonlinear Dyn 82:1269–1280

9. Suneel M (2006) Electronic circuit realization of the logistic map. Sadhana 31:69–78
10. English LQ, Zeng Z, Mertens D (2015) Experimental study of synchronization of coupled electrical self-oscillators and comparison to the Sakaguchi–Kuramoto model. Phys Rev E 92:052912
11. Frøyland J (1983) Some symmetric, two-dimensional, dissipative maps. Phys D 8:423–434
12. Kaneko K (1983) Similarity structure and scaling property of the period-adding phenomena. Prog Theor Phys 69:403–414
13. Yuan J, Tung M, Feng DH, Narducci LM (1983) Instability and irregular behavior of coupled logistic equations. Phys Rev A 28:1662–1666
14. Buskirk R, Jeffries C (1985) Observation of chaotic dynamics of coupled nonlinear oscillators. Phys Rev A 31:3332–3357
15. Sakaguchi H, Tomita K (1987) Bifurcations of the coupled logistic map. Prog Theor Phys 78:305–315
16. Satoh K (1991) Quasiperiodic route to chaos in a coupled logistic map. J Phys Soc Jpn 60:718–719
17. Reick C, Mosekilde E (1995) Emergence of quasiperiodicity in symmetrically coupled, identical period-doubling systems. Phys Rev E 52:1418–1435
18. Bezruchko BP, Seleznev EP (1997) Basins of attraction for chaotic attractors in coupled systems with period-doubling. Tech Phys Lett 23:144–146
19. Anishchenko VS (1989) Dynamical chaos in physical systems. Teubner, Leipzig
20. Gyllenberg M, Soderbacka G, Ericsson S (1992) Does migration stabilize local population dynamics? Analysis of a discrete metapopulation model. Math Biosci 118:25
21. Bezruchko BP, Prokhorov MD, Seleznev Y (1996) Features of the parameter space structure for a system of two coupled nonautonomous nonisochronous oscillators. Pisa Zh Tekh Fiz 22:61
22. Ferretti A, Rahman NK (1998) A study of coupled logistic map and its applications in chemical physics. Chem Phys 119(2):275–288
23. Lloyd AL (1995) The coupled logistic map: a simple model for the effects of spatial heterogeneity on population dynamics. J Theor Biol 173:217–230
24. Kaneko K (1983) Transition from torus to chaos accompanied by frequency lockings with symmetry breaking. Prog Theor Phys 69:1427–1442
25. Hidetsugu S, Kazuhisa T (1987) Bifurcations of the coupled logistic map. Prog Theor Phys 78:305–315
26. Glass L, Goldberger AL, Courtemanche M, Shrier A (1987) Nonlinear dynamics, chaos and complex cardiac arrhythmias. Proc R Soc Lond 413:9–26
27. May R (1987) Chaos and the dynamics of biological populations. Nucl Phys B Proc Suppl 2:225–245
28. Fan M, Agarwal S (2002) Periodic solutions of nonautonomous discrete predator-prey system of Lotka–Volterra type. Appl Anal 81:801–812
29. Jing ZJ, Yang JP (2006) Bifurcation and chaos in discrete-time predator–prey system. Chaos Solitons Fractals 27:259–277
30. Liu X, Xiao D (2007) Complex dynamic behaviors of a discrete-time predator–prey system. Chaos Solitons Fractals 32:80–94
31. Braza PA (2012) Predator prey dynamics with square root functional responses. Nonlinear Anal Real World Appl 13:1837–1843
32. Robinson RC (2004) An introduction to dynamical systems: continuous and discrete. Pearson Prentice Hall, Upper Saddle River
33. Salman SM, Yousef AM, Elsadany AA (2015) Stability, bifurcation analysis and chaos control of a discrete predator–prey system with square root functional response. Chaos Solitons Fractals 93:20–31
34. Elabbasy EM, Elsadany AA, Zhang Y (2014) Bifurcation analysis and chaos in a discrete reduced Lorenz system. Appl Math Comput 228:184–194
35. Solak E, Cokal C (2008) Cryptanalysis of a cryptosystem based on discretized two-dimensional chaotic maps. Phys Lett A 372:6922–6924
36. Han F, Hu J, Yu X, Wang Y (2007) Fingerprint images encryption via multi-scroll chaotic attractors. Appl Math Comput 185:931–939
37. Xie V, Zujun L, Hui W (2007) An image information hiding algorithm based on chaotic permutation. J Inf Secur Commun 6:187–191
38. Hogg T, Huberman BA (1984) Generic behavior of coupled oscillators. Phys Rev A 29:275–281
39. Savi MA (2007) Effects of randomness on chaos and order of coupled logistic maps. Phys Lett A 364:389–395
40. Pisarchik AN, Bashkirtseva I, Ryashko L (2017) Chaos can imply periodicity in coupled oscillators. Europhys Lett 117:40005
41. Bashkirtseva I, Ryashko L (2020) Stochastic deformations of coupling-induced oscillatory regimes in a system of two logistic maps. Phys D Nonlinear Phenom 411:132589
42. Alun LL (1995) The coupled logistic map: a simple model for the effects of spatial heterogeneity on population dynamics. J Theor Biol 173:217–230
43. Zhusubaliyev ZT, Mosekilde E (2009) Multilayered tori in a system of two coupled logistic maps. Phys Lett A 373:946–951
44. Luo ACJ (2012) Regularity and complexity in dynamical systems. Springer, New York
45. Khan A, Ma J, Xiao D (2016) Bifurcations of a two-dimensional discrete time plant-herbivore system. Commun Nonlinear Sci Numer Simul 39:185–198
46. Lifang C, Hongjun C (2016) Bifurcation analysis of a discrete-time ratio-dependent predator–prey model with Allee Effect. Commun Nonlinear Sci Numer Simul 38:288–302
47. Dongpo H, ongjun C (2015) Bifurcation and chaos in a discrete-time predator-prey system of Holling and Leslie type. Commun Nonlinear Sci Numer Simul 22:702–715
48. Dejun F, Junjie W (2009) Bifurcation analysis of discrete survival red blood cells model. Commun Nonlinear Sci Numer Simul 14:3358–3368
49. Sohel Rana SM (2015) Bifurcation and complex dynamics of a discrete-time predator–prey system. Comput Ecol Softw 5:222–238
50. Kuznetsov YA (2004) Elements of applied bifurcation theory. Applied Mathematical Sciences. Springer, New York
51. Wiggins S (1990) An introduction to applied nonlinear dynamics and chaos. Springer, New York
52. Franzke CLE, ÓKane TJ, Berner J, Williams PD, Lucarini V (2015) Stochastic climate theory and modeling. WIREs Clim Change 6:63–78
53. Brittona T, Houseb T, Lloydc AL, Mollisone D, Rileyf S, Trapmana P (2015) Five challenges for stochastic epidemic models involving global transmission. Epidemics 10:54–57
54. Akhlaghi MI, Dogariu A (2015) Stochastic characterization of optical scattering potentials. In: Frontiers in Optics, Optical Society of America, pp. FTh4D-5
55. Anishchenko VS, Neiman AB, Moss F, Shimansky-Geier L (1999) Stochastic resonance: noise-enhanced order. Phys Uspekhi 42(1):7
56. Bashkirtseva I, Ryashko L, Tsvetkov I (2010) Sensitivity analysis of stochastic equilibria and cycles for the discrete dynamic systems. Dyn Contin Discrete Impuls Syst Ser A Math Anal 17(4):501–515
57. Bashkirtseva I, Ryashko L (2013) Stochastic sensitivity analysis of noise-induced intermittency and transition to chaos in one-dimensional discrete-time systems. Phys A Stat Mech Appl 392:295–306

58. Bashkirtseva I, Ryashko L (2014) Stochastic sensitivity of the closed invariant curves for discrete-time systems. Phys A Stat Mech Appl 410:236–43

59. Bashkirtseva I, Ryashko L, Sysolyatina A (2016) Analysis of stochastic effects in Kaldor-type business cycle discrete model. Commun Nonlinear Sci Numer Simul 36:446–456